Hindawi
Mathematical Problems in Engineering
Volume 2021, Article ID 1015367, 20 pages
https://doi.org/10.1155/2021/1015367

Research Article

Optimal Placement of Wind Power Plants in Transmission Power Networks by Applying an Effectively Proposed Metaheuristic Algorithm

Minh Quan Duong,[1] **Thang Trung Nguyen**,[2] **and Thuan Thanh Nguyen**[3]

[1]*Department of Electrical Engineering, University of Science and Technology-The University of DaNang, Da Nang 55000, Vietnam*
[2]*Power System Optimization Research Group, Faculty of Electrical and Electronics Engineering, Ton Duc Thang University, Ho Chi Minh City 700000, Vietnam*
[3]*Faculty of Electrical Engineering Technology, Industrial University of Ho Chi Minh City, Ho Chi Minh City 700000, Vietnam*

Correspondence should be addressed to Thang Trung Nguyen; nguyentrungthang@tdtu.edu.vn

Received 7 September 2021; Revised 28 September 2021; Accepted 29 September 2021; Published 12 October 2021

Academic Editor: Yang Li

In this paper, a modified equilibrium algorithm (MEA) is proposed for optimally determining the position and capacity of wind power plants added in a transmission power network with 30 nodes and effectively selecting operation parameters for other electric components of the network. Two single objectives are separately optimized, including generation cost and active power loss for the case of placing one wind power plant (WPP) and two wind power plants (WPPs) at predetermined nodes and unknown nodes. In addition to the proposed MEA, the conventional equilibrium algorithm (CEA), heap-based optimizer (HBO), forensic-based investigation (FBI), and modified social group optimization (MSGO) are also implemented for the cases. Result comparisons indicate that the generation cost and power loss can be reduced effectively, thanks to the suitable location selection and appropriate power determination for WPPs. In addition, the generation cost and loss of the proposed MEA are also less than those from other compared methods. Thus, it is recommended that WPPs should be placed in power systems to reduce cost and loss, and MEA is a powerful method for the placement of wind power plants in power systems.

1. Introduction

Solving optimal power flow problem (OPF) to have the steady and effective states of power systems is considered as the leading priority in operation of power systems. Specifically, the steady state is represented as a state vector and regarded as a set of variables, such as output of active and reactive power from power plants, voltage of generators in power plants, output of reactive power from shunt capacitors, transformers' tap, voltage of loads, and operating current of transmission lines [1–3]. Generally, during the whole process of solving the OPF problem to determine the steady state in power system operation, the mentioned variables are separated into control variables and dependent variables [4, 5]. The output of the reactive power from power plants (Q_G), output of the active power of power plants at slack node (P_{Gs}), voltage of loads (V_L), and current of lines (I_l) are grouped in a dependent variable set [6–10], whereas other remaining variables including tap changer of transformers (Tap_T), output of the active power from the generators excluding that at slack node (P_{Gs}), and output of the reactive power supplied by capacitor banks (Q_{Cap}) are put in a control variable set [11–15]. These control variables are utilized as the input of the Mathpower programme to find the dependent variables. The Mathpower programme is a calculating tool developed based on the Newton–Raphson method to deal with power flow. After having the dependent variable set, it is checked and penalized based on previously known upper bound and lower bound. The violation of the bounds will be considered for the quality of both control and

dependent variable sets [16–20]. These violations are converted into penalty terms and added to objective functions, such as electrical power generation cost (Cost_e), active power loss (P_{loss}), polluted emission (E_m), and load voltage stability index (ID_{sl}).

Recently, the presence of renewable energies has been considered in power systems when the percentages of wind power and solar energy joining into the process of generating electricity become more and more. In that situation, the OPF problem was modified and became more complex than ever. The conventional version of the OPF problem only considers thermal power plants (THPs) as the main source [21–24]. Other modified versions of the OPF problem, both THPs and renewable energies, are power sources. The modified OPF problem is outlined in Figure 1 in which the conventional OPF problem is a part of the figure without variables regarding renewable energies, such as output of active and reactive power of wind power plant (P_w, Q_w), output of active and reactive power of photovoltaic power plants (PVPs) (P_{pv}, Q_{pv}), and location of WPPs and PVPs (L_w, L_{pv}). There are large number of studies proposed to handle the modified OPF problems. These studies can be classified into three main groups. Specifically, the first group solves the OPF problem considering wind power source injecting both active and reactive power into grid. The second group considers the assumption that wind energy sources just generate active power only. The third group considers both wind and solar energies in the process of solving the OPF problem. The applied methods, test systems, objective functions, placed renewable power plants, and compared methods regarding modified OPF problems are summarized in Table 1. All the studies in the table have focused on the placement of wind and photovoltaic power plants to cut electricity generation fuel cost for THPs, and the results were mainly compared to base systems without the contribution of the renewable plants. In addition, other research directions of optimal power flow are without renewable power plants but using reactive power dispatch [50, 51] and using VSC (voltage source converter) based on HVDC (high-voltage direct current) [52, 53]. These studies also achieved the reduction of cost and improved the quality of voltage as expected. If the combination of both using renewable energies and optimal dispatch of reactive power or the combination of using both renewable energies and these converters can be implemented, expected results such as the reduction of cost and power loss and the voltage enhancement can be significantly better.

In recent years, metaheuristic algorithms have been developed widely and applied successfully for optimization problems in engineering. One of the most well-known algorithms is the conventional equilibrium algorithm (CEA) [54], which was introduced in the early 2020. The conventional version was demonstrated more effective than PSO, GWA, GA, GSA, and SSA for a set of fifty-eight mathematical functions with a different number of variables and types. Over the past year and this year, CEA was widely replicated for different optimization problems such as AC/DC power grids [55], loss reduction of distribution networks [56], component design for vehicles [57], and multidisciplinary problem design [58]. However, the performance of CEA is not the most effective among utilized methods for the same problems. Consequently, CEA had been indicated to be effective for large-scale problems, and it needs more improvements [59–62]. Thus, we proposed another version of CEA, called the modified equilibrium algorithm (MEA), and also applied four other metaheuristic algorithms for checking the performance of MEA.

In this paper, the authors solve a modified OPF (MOPF) problem with the placement of wind power plants in an IEEE 30-bus transmission power network. About the number of wind power plants located in the system, two cases are, respectively, one wind power plant (WPP) and two WPPs. About the locations of the WPPs, simple cases are referred to the previous study [47] and other more complicated cases are to determine suitable buses in the system by applying metaheuristic algorithms. It is noted that the study in [47] has only studied the placement of one WPP, and it has indicated the most suitable bus as bus 30 and the most ineffective bus as bus 3. In this paper, we have employed buses 3 and 30 for two separated cases to check the indication of the study [47]. The results indicated that the placement of one WPP at bus 30 can reach smaller power loss and smaller fuel cost than at bus 3. In addition, the paper also investigated the effectiveness of locations by applying MEA and four other metaheuristic algorithms to determine the location. As a result, placing one WPP at bus 30 has reached the smallest power loss and the smallest total fuel cost. For the case of placing two WPPs, buses 30 and 3 could not result in the smallest fuel cost and the smallest power loss. Buses 30 and 5 are the best locations for the minimization of fuel cost, while buses 30 and 24 are the best locations for the minimization of power loss. Therefore, the main contribution of the study regarding the electrical field is determining the best locations for the best power loss and the best total cost.

All study cases explained above are implemented by the proposed MEA and four existing algorithms published in 2020, including conventional equilibrium algorithm (CEA) [54], heap-based optimizer (HBO) [63], forensic-based investigation (FBI) [64], and modified social group optimization (MSGO) [65]. As a result, the best locations leading to the smallest cost and smallest loss are obtained by MEA. Thus, the applications of the four recent algorithms and the proposed MEA aim to introduce a new algorithm and show their effectiveness to readers in solving the MOPF problem. Readers can give evaluations and decide if the algorithms are used for their own optimization problems, which maybe in electrical engineering or other fields. The major contributions of the paper are summarized again as follows:

(1) Find the best locations for placing wind power plants in the IEEE 30-bus transmission power gird.

(2) The added wind power plants and other found parameters of the system found by MEA can reach the smallest power loss and smallest total cost.

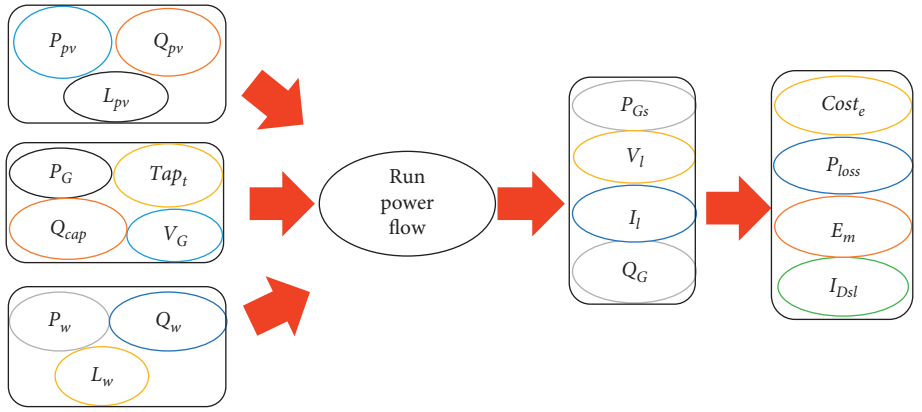

Figure 1: Configuration of the modified OPF problem in the presence of renewable energies.

Table 1: The summary of studies proposed to solve the modified OPF problem considering renewable energies.

Reference	Method	Applied system	Renewable energy	Compared methods
[25]	BFA	30 nodes	Wind (P, Q)	GA
[26]	MBFA	30 nodes	Wind (P, Q)	ACA
[27]	HABC	30 nodes	Wind (P, Q)	ABA
[28]	MCS	30, 57 nodes	Wind (P, Q)	MPSO
[29]	HA	30 nodes	Wind (P, Q)	PSO
[30]	MFO	30 nodes	Wind, solar (P, Q)	GWA, MVA, IMA
[31]	AFAPA	30, 75 nodes	Wind (P)	APO, BA
[32]	KHA	30, 57 nodes	Wind (P)	ALPSO, DE, RCGA
[33]	GSO	300 nodes	Wind (P)	NSGA-II
[34]	MHGSPSO	30, 57 nodes	Wind (P, Q)	MSA, GWA, WA
[35]	BSA	30 nodes	Wind, solar (P)	—
[36]	IMVA	30 nodes	Wind, solar (P, Q)	PSO, MVA, NSGA-II
[37]	PSO	39 nodes	Wind, solar (P)	PSO variants
[38]	NSGA-II	30, 118 nodes	Wind, solar (P)	—
[39]	MFA	30 nodes	Wind, solar (P, Q)	MDE
[40]	GWO	30, 57 nodes	Wind, solar (P)	GA, PSO, CSA1, MDE, ABA
[41]	BWOA, ALO, PSO GSA, MFA, BMA	30 nodes	Wind, solar (P, Q)	—
[42]	FPA	IEEE 30-bus	Wind, solar (P)	—
[43]	APDE	IEEE 30-bus	Wind, solar (P, Q)	—
[44]	HGTPEA	30 nodes	Wind, solar (P)	—
[45]	HGNIPA	118 nodes	Wind, solar (P, Q)	—
[46]	NDSGWA	30 nodes	Wind, solar (P)	MDE
[47]	JYA	30 nodes	Wind, solar (P)	—
[48]	HSQTIICA	30 nodes	DG (P, Q)	IICA
[49]	MJYA	30, 118 nodes	Wind (P)	MSA, ABA, CSA, GWA, BSA

(3) Introduce four existing algorithms developed in 2020 and a proposed MEA. In addition, the performance of these optimization tools is shown to readers for deciding if these tools are used for their applications.

(4) Provide MEA, the most effective algorithm among five applied optimization tools for the MOPF problem.

The organization of the paper is as follows. Two single objectives and a considered constraint set are presented in Section 2. The configuration of CEA for solving a sample optimization problem and then modified points of MEA are clarified in detail in Section 3. Section 4 summarizes the computation steps for solving the modified OPF problem by using MEA. Section 5 presents results obtained by the proposed MEA and other methods such as JYA, FBI, HBO, and MSGO. Finally, conclusions are given in Section 6 for stating achievements in the paper.

2. Objective Functions and Constraints of the Modified OPF Problem

2.1. Objective Functions

2.1.1. Minimization of Electricity Generation Cost. In this research, the first single objective is considered to be electricity generation cost of all thermal generators. At generator nodes, where thermal units are working, the cost is the most

important factor in optimal operation of the distribution power networks, and it should be low reasonably as the following model. The total cost is formulated by

$$\mathrm{EGC} = \sum_{i=1}^{N_{TG}} \mathrm{FE}_{TGi}\left(P_{TGi}\right), \tag{1}$$

where FE_{TGi} is the fuel cost of the ith thermal unit and calculated as follows:

$$\mathrm{FE}_{TGi}\left(P_{TGi}\right) = \mu_{1i} + \mu_{2i}P_{TGi} + \mu_{3i}\left(P_{TGi}\right)^2. \tag{2}$$

2.1.2. Minimization of Active Power Loss. Minimizing active power loss (APL) is a highly important target in transmission line operation. In general, reactive power loss of transmission power networks is very significant due to a high number of transmission lines with high operating current. If the loss can be minimized, the energy loss and the energy loss cost are also reduced accordingly. The loss can be obtained by different ways as follows:

$$\begin{aligned}
\mathrm{APL} &= \sum_{q=1}^{N_{Br}} 3.I_q^2.R_q,\\
\mathrm{APL} &= \sum_{i=1}^{N_{TG}} P_{TGi} - \sum_{i=1}^{N_n} P_{rqi},\\
\mathrm{APL} &= \sum_{x=1}^{N_n} \sum_{\substack{y=1,\\ x\neq y}}^{N_n} Y_{xy}\left[U_x^2 + V_y^2 - 2U_xU_y\,\cos\left(\varphi_x - \varphi_y\right)\right].
\end{aligned} \tag{3}$$

2.2. Constraints

2.2.1. Physical Constraints regarding Thermal Generators. In the operating process of thermal generators, three main constraints need to be supervised strictly consisting of the limitation of real power output, the limitation of reactive power output, and the limitation of the voltage magnitude. The violation of any limitations as mentioned will cause damage and insecure status in whole system substantially. Thus, the following constraints should be satisfied all the time:

$$\begin{aligned}
P_{TGi}^{\min} \le P_{TGi} \le P_{TGi}^{\max}, &\quad \text{with } i = 1, \ldots, \mathrm{NTG},\\
Q_{TGi}^{\min} \le Q_{TGi} \le Q_{TGi}^{\max}, &\quad \text{with } i = 1, \ldots, \mathrm{NTG},\\
U_{TGi}^{\min} \le U_{TGi} \le U_{TGi}^{\max}, &\quad \text{with } i = 1, \ldots, \mathrm{NTG}.
\end{aligned} \tag{4}$$

2.2.2. The Power Balance Constraint. The power balance constraint is the relationship between source side and consumption side in which sources are TUs and renewable energies, and consumption side is comprised of loads and loss on lines. The balance status is established when the amount of power supplied by thermal generators equals to the amount of power required by load plus the loss.

Active power equation at each node x is formulated as follows:

$$P_{TGx} - P_{rqx} = U_x \sum_{y=1}^{N_n} U_y\left[Y_{xy}\cos\left(\varphi_x - \varphi_y\right) + X_{xy}\sin\left(\varphi_x - \varphi_y\right)\right]. \tag{5}$$

For the case that wind turbines supply electricity at node x, the balance of the active power is as follows:

$$P_{TGx} + P_{\mathrm{Wind}x} - P_{rqx} = U_x \sum_{y=1}^{N_n} U_y\left[Y_{xy}\cos\left(\varphi_x - \varphi_y\right) + X_{xy}\sin\left(\varphi_x - \varphi_y\right)\right], \tag{6}$$

where $P_{\mathrm{Wind}x}$ is the power generation of wind turbines at node x and limited by the following constraint:

$$P_{\mathrm{Wind}}^{\min} \le P_{\mathrm{Wind}x} \le P_{\mathrm{Wind}}^{\max}. \tag{7}$$

Similarly, reactive power is also balanced at node x as the following model:

$$Q_{TGx} + Q_{\mathrm{Com}x} - Q_{rqx} = U_x \sum_{y=1}^{N_n} U_y\left[Y_{xy}\sin\left(\varphi_x - \varphi_y\right) - X_{xy}\cos\left(\varphi_x - \varphi_y\right)\right], \tag{8}$$

where

$$Q_{\mathrm{Com}x}^{\min} \le Q_{\mathrm{Com}x} \le Q_{\mathrm{Com}x}^{\max}, \quad \text{with } i = 1, \ldots, N_{Com}. \tag{9}$$

For the case that wind turbines are placed at node x, the reactive power is also supplied by the turbine as the role of thermal generators. As a result, the reactive power balance is as follows:

$$Q_{TGx} + Q_{\text{Wind}x} + Q_{\text{Com}x} - Q_{rqx} = U_x \sum_{y=1}^{N_n} U_y \left[Y_{xy} \sin\left(\varphi_x - \varphi_y\right) - X_{xy} \cos\left(\varphi_x - \varphi_y\right) \right], \in \tag{10}$$

where $Q_{\text{Wind}x}$ is the reactive power generation of wind turbines at node x and is subject to the following constraint:

$$Q_{\text{Wind}}^{\min} \le Q_{\text{Wind}x} \le Q_{\text{Wind}}^{\max}. \tag{11}$$

2.2.3. Other Inequality Constraints. These constraints are related to operating limits of electric components such as lines, loads, and transformers. Lines and loads are dependent on other operating parameters of other components like TUs, wind turbines, shunt capacitors, and transformers. However, operating values of lines and loads are very important for a stable operating status of networks. If the components are working beyond their allowable range, networks are working unstably, and fault can occur in the next phenomenon. Thus, the operating parameters of loads and lines must be satisfied as shown in the following models:

$$\begin{aligned} U_{LN}^{\min} \le U_{LNt} \le U_{LN}^{\max}, &\quad \text{with } t = 1, \ldots, N_{LN}, \\ S_{Brq} \le S_{Br}^{\max}, &\quad \text{with } q = 1, \ldots, N_{Br}. \end{aligned} \tag{12}$$

In addition, transformers located at some nodes need to be tuned for supplying standard voltage within a working range. The voltage regulation is performed by setting tap of transformers satisfying the following constraint:

$$\text{Tap}^{\min} \le \text{Tap}_i \le \text{Tap}^{\max}, \quad \text{with } i = 1, \ldots, N_T. \tag{13}$$

3. The Proposed Modified Equilibrium Algorithm (MEA)

3.1. Conventional Equilibrium Algorithm (CEA). CEA was first introduced and applied in 2020 for solving a high number of benchmark functions. The method was superior to popular and well-known metaheuristic algorithms, but its feature is simple with one technique of newly updating solutions and one technique of keeping promising solutions between new and old solutions.

The implementation of CEA for a general optimization problem is mathematically presented as follows.

3.1.1. The Generation of Initial Population. CEA has a set of N_1 candidate solutions similar to other metaheuristic algorithms. The solution set needs to define the boundaries in advance, and then it must be produced in the second stage. The set of solution is represented by $Z = [Z_d]$, where $d = 1, \ldots, N_1$, and the fitness function of the solution set is represented by $\text{Fit} = [\text{Fit}_d]$, where $d = 1, \ldots, N_1$.

To produce an initial solution set, control variables included in each solution and their boundaries must be, respectively, predetermined as follows:

$$\begin{aligned} Z_d &= \left[z_{j\,d} \right]; \quad j = 1, \ldots, N_2; d = 1, \ldots N_1, \\ Z_{\text{low}} &= \left[z_{j\text{low}} \right]; \quad j = 1, \ldots, N_2, \\ Z_{\text{up}} &= \left[z_{j\text{up}} \right]; \quad j = 1, \ldots, N_2, \end{aligned} \tag{14}$$

where N_2 is the control variable number, z_{jd} is the jth variable of the dth solution, Z_{low} and Z_{up} are lower and upper bounds of all solutions, respectively, and $z_{j\text{low}}$ and $z_{j\text{up}}$ are the minimum and maximum values of the jth control variable, respectively.

The initial solutions are produced within their bounds Z_{low} and Z_{up} as follows:

$$Z_d = Z_{\text{low}} + r_1 \cdot \left(Z_{\text{up}} - Z_{\text{low}} \right); \quad d = 1, \ldots, N_1. \tag{15}$$

3.1.2. New Update Technique for Variables. The matrix fitness fit is sorted to select the four best solutions with the lowest fitness values among the available set. The solution with the lowest fitness is set to $Z_{b1,}$ while the second, third, and fourth best solutions with the second, third, and fourth lowest fitness functions are assigned to Z_{b2}, Z_{b3}, and Z_{b4}. In addition, another solution, which is called the middle solution (Z_{mid}) of the four best solutions, is also produced by

$$Z_{\text{mid}} = \frac{\left(Z_{b1} + Z_{b2} + Z_{b3} + Z_{b4} \right)}{4}. \tag{16}$$

The four best solutions and the middle solution are grouped into the solution set Z_{5b} as follows:

$$Z_{5b} = \left\{ Z_{b1}, Z_{b2}, Z_{b3}, Z_{b4}, Z_{\text{mid}} \right\}. \tag{17}$$

As a result, the new solution $Z_{d\text{new}}$ of the old solution Z_d is determined as follows:

$$Z_{d\text{new}} = Z_{5brd} + M \cdot \left(Z_d - Z_{5brd} \right) + \frac{K \times M}{r_2} \left(1 - M \right). \tag{18}$$

In the above equation, Z_{5brd} is a randomly chosen solution among five solutions of Z_{5b} in equation (17), whereas M and K are calculated by

$$M = 2\text{sign}\left(r_3 - 0.5 \right) \left(\frac{1}{e^{A.\text{Iter}}} - 1 \right), \tag{19}$$

$$K = K_0 \cdot \left(Z_{5brd} - r_4 \cdot Z_d \right), \tag{20}$$

$$A = \left(1 - \frac{\text{Iter}}{N_3} \right)^{\left(\text{Iter}/N_3 \right)}, \tag{21}$$

$$K_0 = \begin{cases} 0, & \text{if } \& \, r_5 < 0.5, \\ \dfrac{r_6}{2}, & \& \text{otherwise}. \end{cases} \tag{22}$$

3.1.3. New Solution Correction. The new solution $Z_{d\text{new}}$ is a set of new control variables $z_{jd,,\text{new}}$ that can be beyond the minimum and maximum values of control variables. It means $z_{jd,,\text{new}}$ may be either higher than $z_{j\text{up}}$ or smaller than $z_{j\text{low}}$. If one out of the two cases happens, each new variable $z_{jd,,\text{new}}$ must be redetermined as follows:

$$z_{j\,d,\text{new}} = \begin{cases} z_{jd,\text{new}}, & \text{if } z_{j\text{low}} \le z_{jd,\text{new}} \le z_{j\text{up}}, \\ z_{j\text{low}}, & \text{if } z_{j\text{low}} > z_{jd,\text{new}}, \\ z_{j\text{up}}, & \text{if } z_{jd,\text{new}} > z_{j\text{up}}. \end{cases} \tag{23}$$

After correcting the new solutions, the new fitness function is calculated and assigned to $\text{Fit}_{d\text{new}}$.

3.1.4. Selection of Good Solutions. Currently, there are two solution sets, one old set and one new set. Therefore, it is important to retain higher quality solutions so that the retained solutions are equal to N_1. This task is accomplished by using the following formula:

$$Z_d = \begin{cases} Z_{d\text{new}}, & \text{if } \text{Fit}_d > \text{Fit}_{d\text{new}}, \\ Z_{d\text{new}}, & \text{if } \text{Fit}_d = \text{Fit}_{d\text{new}}, \\ Z_d, & \text{else}, \end{cases} \tag{24}$$

$$\text{Fit}_d = \begin{cases} \text{Fit}_{d\text{new}}, & \text{if } \text{Fit}_d > \text{Fit}_{d\text{new}}, \\ \text{Fit}_{d\text{new}}, & \text{if } \text{Fit}_d = \text{Fit}_{d\text{new}}, \\ \text{Fit}_d, & \text{else}. \end{cases} \tag{25}$$

3.1.5. Termination Condition. CEA will stop updating new control variables when the computation iteration reaches the maximum value N_3. In addition, the best solution and its fitness are also reported.

3.2. The Proposed MEA. The proposed MEA is a modified variant of CEA by using a new technique for updating new control variables. From equation (18), it sees that CEA only chooses search spaces around the four best solutions and the middle solution (i.e., $Z_{b1}, Z_{b2}, Z_{b3}, Z_{b4}, Z_{\text{mid}}$) for updating decision variables whilst from search spaces nearby from the fifth best solution to the worst solution are skipped intentionally. In addition, the strategy has led to the success of CEA with better performance than other metaheuristics. However, CEA cannot reach a higher performance because it is coping with two shortcomings as follows:

(1) The first shortcoming is to pick up one out of five solutions in the set Z_{5b} randomly. The search spaces may be repeated more than once and even too many times. Therefore, promising search spaces can be exploited ineffectively or skipped unfortunately.

(2) The second shortcoming is to use two update steps including $M \times (Z_{b1} - Z_d)$ and $(K \times M/r_2)(1 - M)$, which are decreased when the computation iteration is increased. Especially, the steps become zero at final computation iterations. In fact, parameter A in equation (21) becomes 0 when the current iteration is equal to the maximum iteration N_3. If we substitute $A = 0$ into equation (19), M becomes 0.

Thus, the proposed MEA is reformed to eliminate the above drawbacks of CEA and reach better results as solving the OPF problem with the presence of wind energy. The two proposed formulas for updating new decision variables are as follows:

$$Z_{d\text{new1}} = Z_d + M(Z_{b1} - Z_d) + r_7(Z_{r1} - Z_{r2}), \tag{26}$$

$$Z_{d\text{new2}} = Z_{b1} + M(Z_d - Z_{b1}) + r_8(Z_{r3} - Z_{r4}). \tag{27}$$

The two equations above are not applied simultaneously for the same old solution i. Either equation (26) or equation (27) is used for the dth new solution. $Z_{d\text{new1}}$ in equation (26) is applied to update Z_d if Z_d has better fitness than the medium fitness of the population, i.e., $\text{Fit}_d < \text{Fit}_{\text{mean}}$. For the other case, i.e., $\text{Fit}_d \ge \text{Fit}_{\text{mean}}$, $Z_{d\text{new2}}$ in equation (27) is determined.

4. The Application of the Proposed MEA for OPF Problem

4.1. Generation of Initial Population. The problem of placing wind turbines in the transmission power network is successfully solved by using decision variables as follows: the active power generation and voltage of thermal generators (excluding power generation at slack node), generation of capacitors, tap of transformer, and position, active and reactive power of wind turbines. Hence, Z_d is comprised of the following decision variables: P_{TGi} ($i = 2, \ldots, N_{TG}$); U_{TGi} ($i = 1, \ldots, N_{TG}$); Q_{Comi} ($i = 1, \ldots, N_{Com}$); Tap_i ($i = 1, \ldots, N_T$); $P_{\text{Wind}x}$ ($x = 1, \ldots, N_W$); $Q_{\text{Wind}x}$ ($x = 1, \ldots, N_W$); and $L_{\text{Wind}x}$ ($x = 1, \ldots, N_W$).

The decision variables are initialized within their lower bound Z_{low} and upper bound Z_{up} as shown in Section 2.

4.2. The Calculation of Dependent Variables. Before running Mathpower program, control variables of wind turbines including active power, reactive power, and location are collected to calculate the new values of loads at the placement of the wind turbines. Then, the data of the load must be changed and then added in the input data of Mathpower program. Finally, other remaining decision variables are added to Mathpower program and running power flow for obtaining dependent variables including P_{TG1}; Q_{TGi} ($i = 1, \ldots, N_{TG}$); U_{LNt} ($t = 1, \ldots, N_{LN}$); and S_{Brq} ($q = 1, \ldots, N_{Br}$).

4.3. Solution Evaluation. The quality of solution Z_d is evaluated by calculating the fitness function. Total cost and total active power loss are two single objectives, while the violations of dependent variables are converted into penalty values [66].

4.4. Implementation of MEA for the Problem. In order to reach the optimal solution for the OPF problem with the presence of wind turbines, the implementation of MEA is shown in the following steps and is summarized in Figure 2.

Step 1: select population N_1 and maximum iteration N_2.

Step 2: select and initialize decision variables for the population as shown in Section 4.1.

Step 3: collect variables of wind turbines and tune loads.

Step 4: running Mathpower for obtaining dependent variables shown in Section 4.2.

Step 5: evaluate quality of obtained solutions as shown in Section 4.3.

Step 6: select the best solution Z_{b1} and set Iter = 1.

Step 7: select four random solutions Z_{r1}, Z_{r2}, Z_{r3}, and Z_{r4}.

Step 8: calculate the mean fitness of the whole population.

Step 9: produce new solutions. *If* $\text{Fit}_d < \text{Fit}_{\text{mean}}$, apply equation (26) to produce new solution. Otherwise, apply equation (27) to produce new solutions.

Step 10: correct new solutions using equation (23).

Step 11: collect variables of wind turbines and tune loads.

Step 12: running Mathpower for obtaining dependent variables shown in Section 4.2.

Step 13: evaluate quality of obtained solutions as shown in Section 4.3.

Step 14: select good solutions among old population and new population using equations (24) and (25).

Step 15: select the best solution Z_{b1}.

Step 16: if Iter = N_3, stop the search process and print the optimal solution. Otherwise, set Iter to Iter + 1 and back to Step 7.

5. Numerical Results

In this section, MEA together with four other methods including FBI, HBO, MSGO, and CEA are applied for placing WPPs on the IEEE 30-node system with 6 thermal generators, 24 loads, 41 transmission lines, 4 transformers, and 9 shunt capacitors. The ssingle line diagram of the system is shown in Figure 3 [67]. Different study cases are carried out as follows:

Case 1: minimization of generation cost

Case 1.1: place one wind power plant at nodes 3 and 30, respectively
Case 1.2: place one WPP at one unknown node
Case 1.3: place two wind power plants at two nodes

Case 2: minimization of power loss

Case 2.1: place one wind power plant at nodes 3 and 30, respectively
Case 2.2: place one WPP at one unknown node
Case 2.3: place two wind power plants at two nodes

The five methods are coded on Matlab 2016a and run on a personal computer with a processor of 2.0 GHz and 4.0 GB of RAM. For each study case, fifty independent runs are performed for each method, and the collected results are minimum, mean, maximum, and standard deviation values.

5.1. Electricity Generation Cost Reduction

5.1.1. Case 1.1: Place One Wind Power Plant at Nodes 3 and 30, Respectively. In this study case, one power plant is, respectively, placed at node 3 and node 30 for comparison of the effectiveness of the placement position. As shown in [47], node 30 and node 3 are the most effective and ineffective locations for placing renewable energies. The found results from the five applied and JYA methods for the placement of WPPs at node 3 and node 30 are reported in Tables 2 and 3, respectively. Table 2 shows that the best cost of MEA is \$764.33, while that of other methods is from \$764.53 (CEA) to \$769.963 (JYA). Exactly, MEA reaches better cost than others by from \$0.2 to \$5.633. Table 3 has the same features since MEA reaches the lowest cost of \$762.53, while that from others is from \$762.62 (CEA) to \$768.039 (JYA). In addition, MEA can obtain less cost than others by from \$0.09 to \$5.509. The best cost indicates that MEA is the most powerful method among all the applied and JYA methods, while the standard deviation (STD) of MEA is the second lowest and it is only higher than that of HBO.

For the effectiveness comparison between node 3 and node 30, it concludes that node 30 is more suitable to place WPPs. In fact, FBA, HBO, MSGO, CEA, MEA, and IAYA [47] can reach less cost for node 30. The cost of the methods is, respectively, \$763.56, \$763.24, \$765.74, \$762.62, \$762.53, and \$768.039 for node 30, but \$764.69, \$764.99, \$766.85, \$764.53, \$764.33, and \$769.963 for node 3.

Figures 4 and 5 show the best run of the applied methods for placing WPPs at node 3 and node 30, respectively. The curves see that MEA is much faster than the other methods even its solution at the 70^{th} iteration is much better than that of others at the final iteration.

5.1.2. Case 1.2: Place One WPP at One Unknown Node. In this section, the location of one WPP together with active and reactive power are determined instead of fixing the location at node 3 and node 30 similar to Case 1.1. Table 4 indicates that MEA can reach better costs and STD than all methods. Table 5 summarizes the results of one WPP for Case 1.1 and Case 1.2. It is recalled that the power factor selection of wind power plant is from 0.85 to 1.0, while the active power is from 0 to 10 MW. For Case 1.2, HBO, CEA, and MEA can find the same location (node 30), while FBI and MSGO can find node 19 and node 26, respectively. Thus, the cost of FBI and MSGO is the worst, while others have better costs. The conclusion is very important to confirm that the renewable energy source placement location in the transmission power network has high impact on the effective operation. Figure 6 shows the best run of applied methods, and it also leads to the conclusion that MEA is the fastest among these methods.

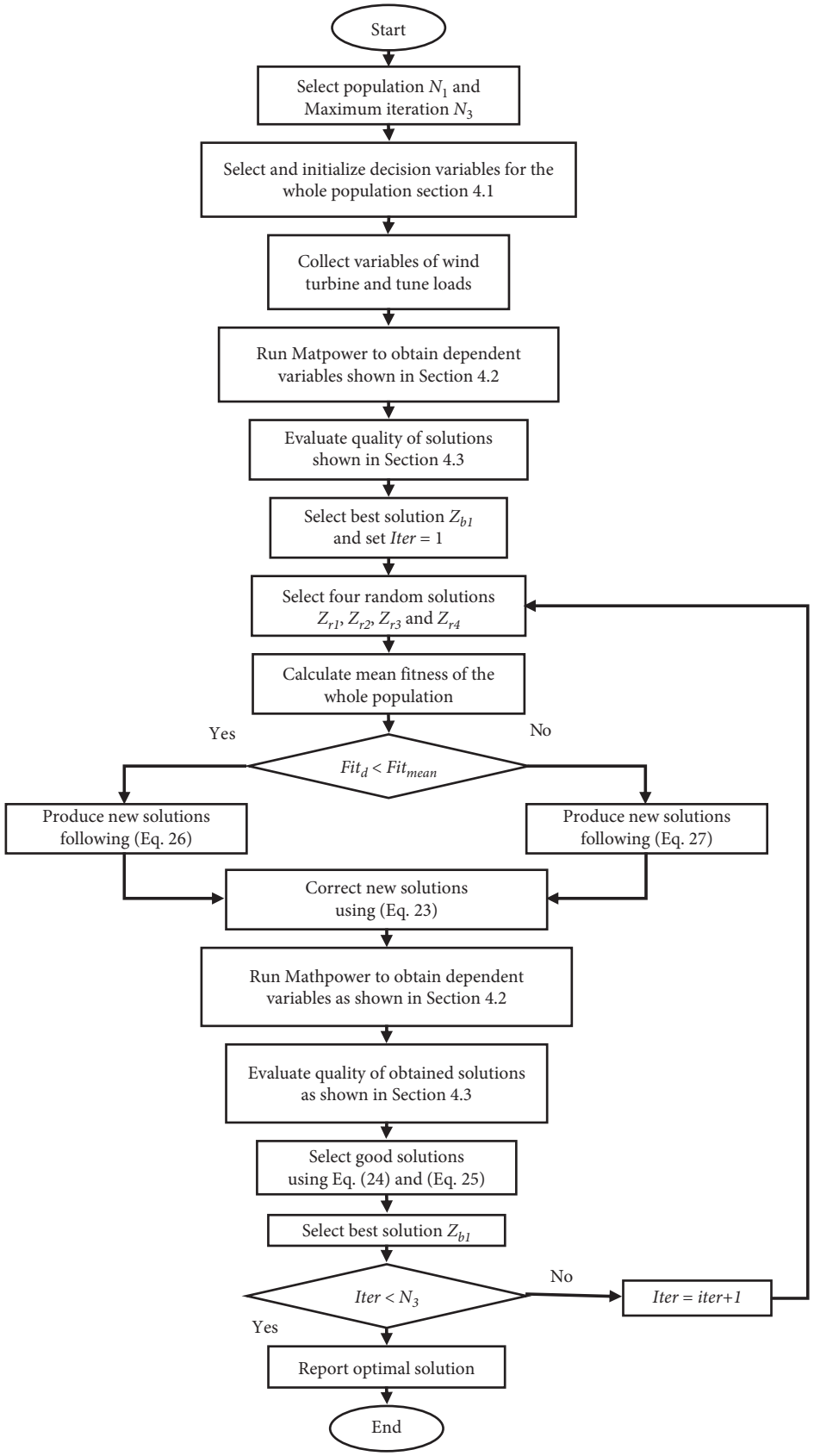

Figure 2: The flowchart of using MEA for solving the modified OPF problem.

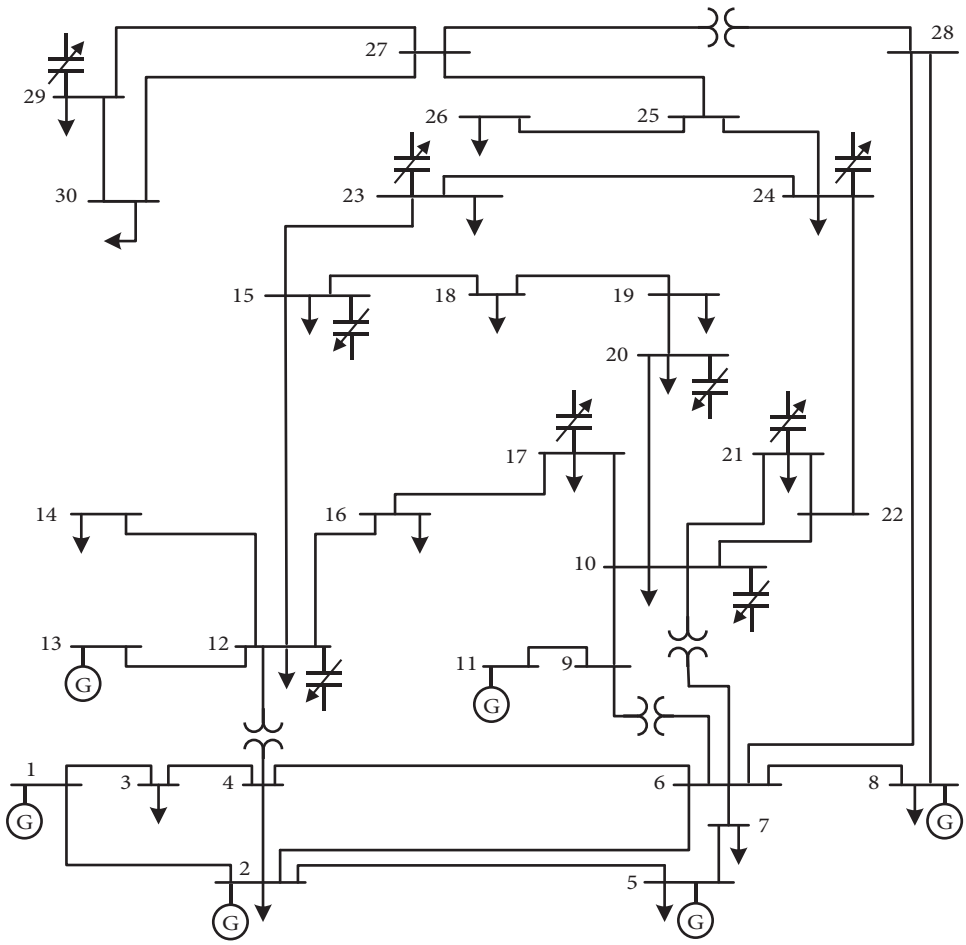

Figure 3: The IEEE 30-node transmission network.

Figure 7 shows the fifty runs obtained by MEA. The black curve shows fifty sorted loss values, while blue bars show the location of the added WPP. In the figure, fifty runs are rearranged by sorting the cost from the smallest to the highest. Accordingly, the location of the runs is also reported. The locations indicate that node 30 is found many times, while other nodes such as 19 and 5 are also found, but the cost of nodes 19 and 5 is much higher than that of node 30.

5.1.3. Case 1.3: Place Two Wind Power Plants at Two Nodes. In this case, five methods are applied to minimize the cost for two subcases, Subcase 1.3.1 with two WPPs at node 3 and node 30 and Subcase 1.3.2 with unknown locations of two WPPs. The results for the two cases are reported in Tables 6 and 7. MEA can reach the lowest cost for the two subcases, which is \$728.15 for Subcase 1.3.1 and \$726.77 for Subcase 1.3.2. It can be seen that the locations at nodes 30 and 3 are not as effective as locations at nodes 30 and 5. In addition to MEA, CEA also finds the same locations at nodes 30 and 5 for Subcase 1.3.2, and CEA reaches the second-best cost behind MEA. FBI, HBO, and MSGO cannot find the same nodes 30 and 5, and they suffer higher cost than CEA and MEA.

Table 2: The results obtained by methods for placing one WPP at node 3.

Method	FBI	HBO	MSGO	CEA	MEA	JYA [47]
Minimum cost (\$/h)	764.69	764.99	766.85	764.53	764.33	769.963
Mean cost (\$/h)	767.23	765.76	782.38	765.95	765.94	—
Maximum cost (\$/h)	772.62	766.71	838.51	768.83	767.91	—
STD	1.87	0.87	15.78	1.05	1.01	—
N_1	10	30	15	30	30	40
N_3	100	100	100	100	100	100

Figure 8 presents the cost and the locations of the two WPPs obtained by 50 runs. The black curve shows fifty values of loss sorted in the ascending order, while the blue and orange bars show the location of the first WPP and the second WPP. All the costs are rearranged from the lowest to the highest values. The figure indicates that the best cost and second-best cost are obtained by placing WPPs at nodes 30 and 5,while the next six best costs are obtained by placing WPPs at nodes 30 and 19. Other worse costs are found by placing the same nodes 30 and 5

Table 3: The results obtained by methods for placing one WPP at node 30.

Method	FBI	HBO	MSGO	CEA	MEA	JYA [47]
Minimum cost ($/h)	763.56	763.24	765.74	762.62	762.53	768.039
Mean cost ($/h)	765.91	764.15	780.02	764.61	764.36	—
Maximum cost ($/h)	769.50	765.82	880.75	766.62	767.88	—
STD	1.61	0.68	22.19	1.28	1.23	—
N_1	10	30	15	30	30	30
N_3	100	100	100	100	100	100

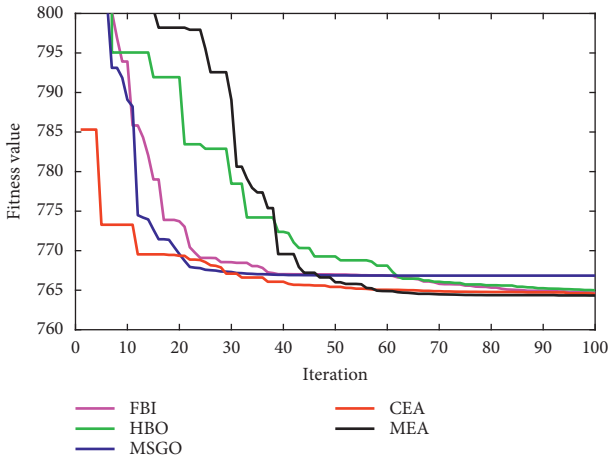

Figure 4: The best runs of methods for the wind power plant placement at node 3.

or nodes 30 and 19. For a few cases, two WPPs are placed at nodes 30 and 24, but their cost is much higher. Clearly, node 30 is the most important, and node 5 is the next important location for supplying additional active and reactive power.

Figures 9 and 10 show the best run of applied methods for Subcases 1.3.1 and 1.3.2, respectively. Figure 9 shows a clear outstanding performance of MEA over other methods since the sixtieth iteration to the last iteration. The cost of MEA at the sixtieth iteration is smaller than that of other methods at the final iteration. Figure 10 also shows that MEA is much faster than FBI, HBO, and MSGO from the 30th iteration to the last iteration. The cost of MEA is always smaller than these methods from the 30th iteration to the last iteration. CEA shows a faster search than MEA from the first to the 80th iteration, but it is still worse than MEA from the 81st iteration to the last iteration. Obviously, MEA has a faster search than others.

5.2. Active Power Loss Reduction

5.2.1. Case 2.1: Place One Wind Power Plant at Nodes 3 and 30, Respectively. In this section, one WPP is, respectively, located at nodes 30 and 3 for reducing power loss. Tables 8 and 9 show the obtained results from 50 trial runs. The loss of MEA

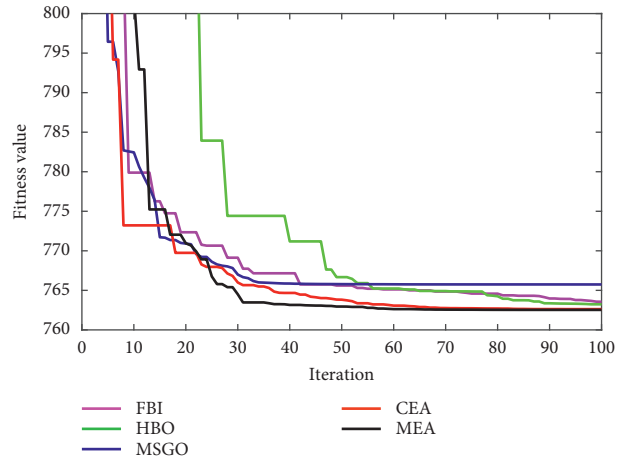

Figure 5: The best runs of methods for the wind power plant placement at node 30.

Table 4: The results obtained by five implemented methods for Case 1.2.

Method	FBI	HBO	MSGO	CEA	MEA
Minimum cost ($/h)	763.96	762.72	765.22	762.89	762.52
Mean cost ($/h)	767.96	764.32	782.08	764.59	763.54
Maximum cost ($/h)	786.95	766.45	869.63	767.68	766.17
STD	4.45	0.96	18.27	1.29	0.94
N_1	10	30	15	30	30
N_3	100	100	100	100	100

is the best for the cases of placing one WPP at node 3 and node 30. The best loss of MEA is 2.79 MW for the placement at node 3 and 2.35 MW for the placement at node 30, while those of others are from 2.8 MW to 3.339 MW for the placement at node 3 and from 2.37 MW to 2.67504 MW for the placement at node 30. On the other hand, all methods can have better loss when placing one WPP at node 30. Clearly, node 30 needs more supplied power than node 3. About the speed of search, Figures 11 and 12 indicate that MEA is much more effective than the other ones since its loss found at the 70th iteration is smaller than that of others at the final iteration.

5.2.2. Case 2.2. Place One WPP at One Unknown Node. In this section, five applied methods are implemented to find the location and power generation of one WPP. Table 10 indicates that all methods have found the same location at node 30, but MEA is still the most effective method with the lowest loss even it is not much smaller than others. The loss of MEA is 2.39 MW, while that of others is from 2.45 MW to 2.7 MW. HBO is still the most stable method with the smallest STD. Figure 13 shows the best run of five methods. In the figure, MSGO has a premature convergence to a local optimum with very low quality, while other methods are searching optimal solutions. CEA seems to have a better search process than MEA from the 1st iteration to the 90th iteration, but then it must adopt a higher loss from the 91st iteration to the last iteration. Figure 14 presents the location and the loss of the proposed MEA for 50 runs. The

Table 5: The optimal solutions obtained by methods for case 1.1 and case 1.2.

Case	Method	FBI	HBO	MSGO	CEA	MEA	JYA [47]
Case 1.1 (place WPP at node 3)	Location of WPP	3	3	3	3	3	3
	Generation of WPP (MW)	9.99	10.00	9.99	10.00	10.00	9.1169
	Power factor of WPP	0.97	0.89	0.88	0.85	0.89	0.85
	Minimum cost ($/h)	764.69	764.99	766.85	764.53	764.33	769.963
Case 1.1 (place one WPP at node 30)	Location of WPP	30	30	30	30	30	30
	Generation of WPP (MW)	9.98	10.00	10.00	10.00	10.00	9.1478
	Power factor of WPP	0.88	0.90	0.99	0.99	1.00	0.85
	Minimum cost ($/h)	763.56	763.24	765.74	762.62	762.53	768.039
Case 1.2 (find the location of WPP)	Location of WPP	19	30	26	30	30	—
	Generation of WPP (MW)	10.00	10.00	10.00	10.00	10.00	—
	Power factor of WPP	0.93	0.97	0.92	0.99	0.95	—
	Minimum cost ($/h)	763.96	762.72	765.22	762.89	762.52	—

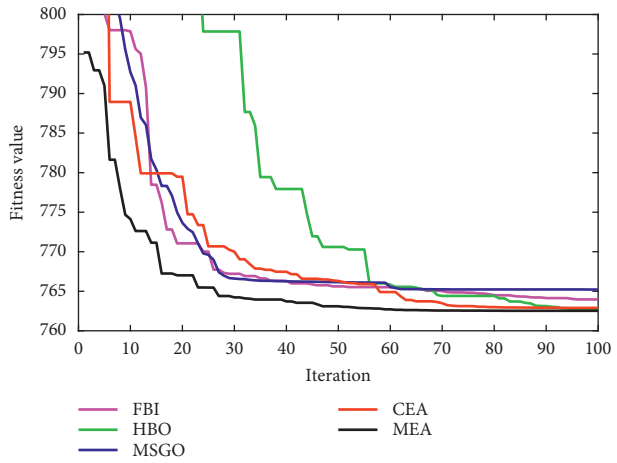

Figure 6: The best run of applied methods for Case 1.2.

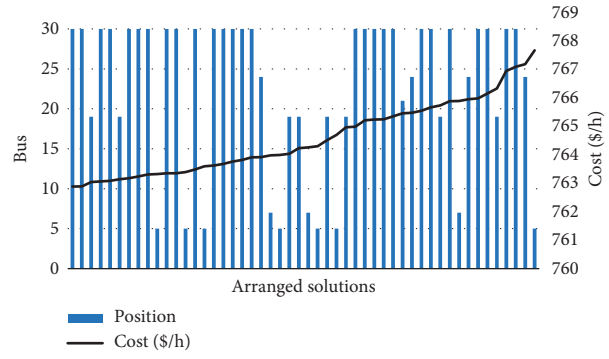

Figure 7: WPP location and cost of 50 rearranged runs obtained by MEA.

rearranged losses from the lowest to the highest indicate that node 30 can reduce the loss at most, while other nodes such as 5, 7, 19, 24, and 26 are not suitable for reducing loss.

5.2.3. Case 2.2. Place Two WPPs at Two Nodes. In this section, Subcase 2.2.1 is to place two WPPs at two predetermined nodes 3 and 30 and Subcase 2.2.2 is to place two WPPs at two random nodes. Tables 11 and 12 show the results for the two studied subcases.

The two tables reveal that MEA can reach the lowest loss for both cases, 2.26 MW for Subcase 2.2.1 and 2.03 MW for Subcase 2.2.2. Clearly, placing WPP at the most effective node (node 30) and the least effective node (node 3) cannot lead to a very good solution of reducing total loss. While, the WPP placement at node 30 and node 24 can reduce the loss from 2.26 to 2.03 MW, which is about 0.23 MW and equivalent to 10.2%. When comparing to CEA, MSGO, HBO, and FBI, the proposed MEA can save 0.02, 0.06, 0.17, and 0.11 MW for Subcase 2.2.1 and 0.02, 0.07, 0.13, and 0.21 MW for Subcase 2.2.2. The mean loss of MEA is also smaller than that of MSGO, HBO, and FBI and only higher than that of CEA. The STD comparison is the same as the mean loss comparison. Figures 15 and 16 show the search procedure of the best run obtained by five applied methods. Figure 15 indicates that MEA can find better parameters for wind power plants and other electrical components than other methods from the 75^{th} iteration to the last iteration. Therefore, its loss is less than that of four remaining methods from the 75^{th} to the last iteration. Figure 16 shows a better search procedure for MEA with less loss than other ones from the 55^{th} iteration to the last iteration. The two figures have the same point that the loss of MEA at the 86^{th} iteration is less than that of CEA at the final iteration. Compared to three other remaining methods, the loss of MEA at the 67^{th} iteration for Subcase 2.2.1 and at the 56^{th} iteration for Subcase 2.2.2 is less than that of these methods at the final iteration. Obviously, MEA is very strong for placing two WPPs in the IEEE 30-bus system.

Figure 17 shows the power loss and the location of the two WPPs for the fifty runs obtained by MEA. The black curve shows fifty sorted loss values, while the blue and orange bars show the location of the first WPP and the second WPP. The view on the bars and the curve sees that node 30 is always chosen, while the second location can be nodes 24, 19, 21, 5, and 4. The best loss and second-best loss are obtained at nodes 30 and 24, while other nodes reach much higher losses.

Table 6: The results obtained by five implemented methods for Subcase 1.3.1.

Method	FBI	HBO	MSGO	CEA	MEA
Minimum cost ($/h)	728.61	728.40	728.80	728.39	728.15
Mean cost ($/h)	731.27	729.73	736.72	731.28	728.74
Maximum cost ($/h)	738.69	731.50	762.72	765.83	730.55
STD	1.89	0.71	7.52	5.13	0.57
N_1	20	60	30	60	60
N_3	100	100	100	100	100
Generation of WPP at node 30 (MW)	9.9731	10	9.9589	10	10
Generation of WPP at node 3 (MW)	9.9693	10	9.9999	9.9858	10
Power factor of WPP at node 30	0.92	0.9004	0.9803	0.9048	0.8857
Power factor of WPP at node 3	0.9782	0.9366	0.9992	0.9838	0.947

Table 7: The results obtained by five implemented methods for Subcase 1.3.2.

Method	FBI	HBO	MSGO	CEA	MEA
Minimum cost ($/h)	728.20	727.41	728.81	726.84	726.77
Mean cost ($/h)	730.67	728.69	731.75	728.17	728.04
Maximum cost ($/h)	733.77	729.89	739.08	730.59	730.35
STD	1.27	0.60	2.20	0.98	0.95
N_1	20	60	30	60	60
N_3	100	100	100	100	100
Locations of WPPs	30, 24	30, 19	24, 19	30, 5	30, 5
Generation of WPPs (MW)	9.95, 9.9623	10, 9.9995	10, 9.9982	10, 10	10, 10
Power factor of WPPs	0.9604, 0.9349	0.9605, 0.9394	0.9418, 0.9135	0.9342, 0.9458	0.9433, 0.8718

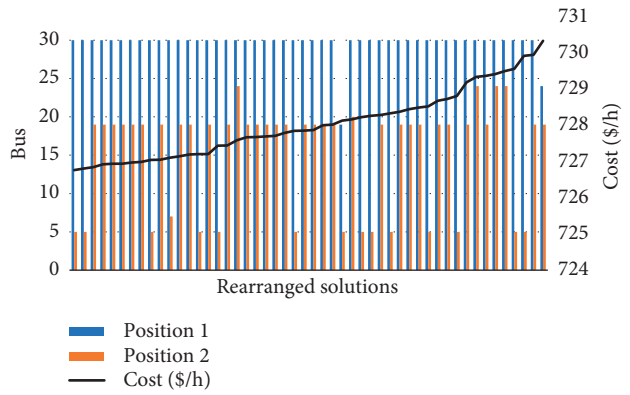

Figure 8: WPP location and cost of 50 rearranged runs obtained by MEA for Subcase 1.3.2.

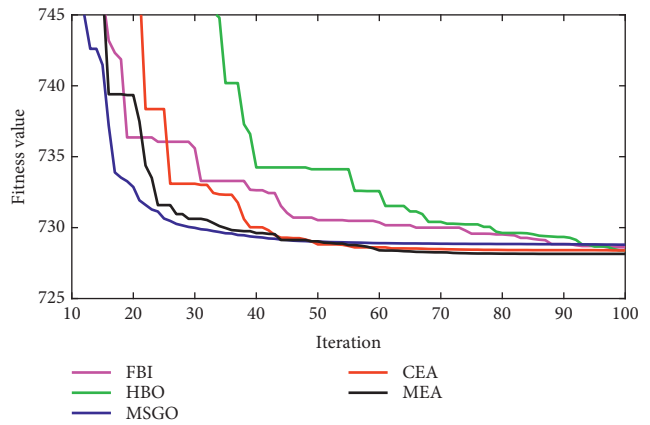

Figure 9: The best run obtained by five applied methods for Subcase 1.3.1.

5.3. Discussion on the Capability of MEA. In this paper, we considered the placement of WPPs on the IEEE 30-node system. The dimension of the system is not high, it is just medium. In fact, among IEEE standard transmission power systems such as IEEE 14-bus system, IEEE 30-bus system, IEEE 57-bus system, IEEE 118-bus system, etc. The considered system is not the largest system, and it has 6 thermal generators, 24 loads, 41 transmission lines, 4 transformers, and 9 shunt capacitors. With the number of power plants, lines, loads, transformers, and capacitors, the IEEE 30-bus system is approximately as large as an area power system in a province. By considering the placement of WPPs, the control variables of WPPs are location, active power, and reactive power. Therefore, there are six control variables regarding two placed WPPs, including two locations, two values of rated power, and two values of reactive power. In addition, other control variables regarding optimal power flow problem are 5 values of active power output for 6 THPs, 6 voltage values for THPs, 4 tap values for transformers, and 9 reactive power output values for shunt capacitors. On the other hand, the dependent variables are 1 value of the active power output for generator at slack node, 6 values of reactive power for THPs, 41 current values of lines, and 24 voltage values of loads. As a result, the total number of control variables for placing two WPPs in the IEEE 30-bus system is 30, and the total number of dependent variables is 72. In the conventional OPF problem, control variables have a high impact on the change of dependent variables, and updating the control variables causes the change of dependent variables. Furthermore, in the modified OPF problem, updating the location and size of WPPs also cause the change of

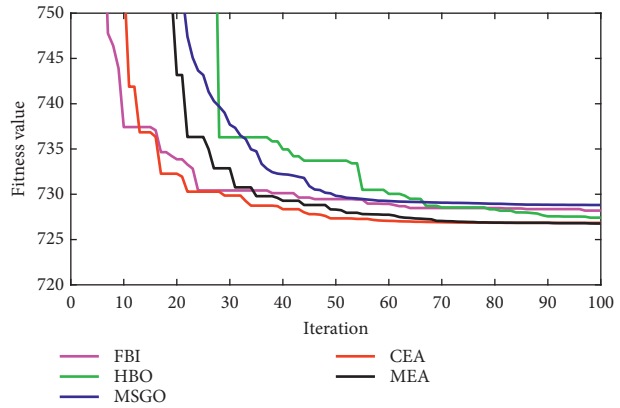

Figure 10: The best run obtained by five applied methods for Subcase 1.3.2.

Table 8: The results obtained by methods as placing one WPP at node 3 for loss reduction.

Method	FBI	HBO	MSGO	CEA	MEA	JYA [47]
Minimum power loss (MW)	2.91	2.87	2.91	2.80	2.79	3.3390
Mean power loss (MW)	3.35	3.08	4.01	3.11	3.10	—
Maximum power loss (MW)	4.68	3.30	6.87	3.40	3.36	—
STD	0.39	0.10	1.09	0.16	0.15	—
Generation of WPP (MW)	9.1505	9.8076	8.9369	9.9559	9.9958	8.2827
Power factor of WPP	0.9601	0.9989	0.974	0.9168	1	0.85

Table 9: The results obtained by methods as placing one WPP at node 30 for loss reduction.

Method	FBI	HBO	MSGO	CEA	MEA	JYA [47]
Minimum power loss (MW)	2.51	2.47	2.43	2.37	2.35	2.67504
Mean power loss (MW)	2.96	2.62	3.23	2.73	2.65	—
Maximum power loss (MW)	4.50	2.85	5.69	3.18	2.97	—
STD	0.43	0.09	0.89	0.17	0.14	—
N_1	10	30	15	30	30	30
N_3	100	100	100	100	100	100
Generation of WPP (MW)	9.1821	9.8257	9.7111	9.9904	9.9853	9.95433
Power factor of WPP	0.9732	0.9947	0.9905	0.9455	0.9914	0.85

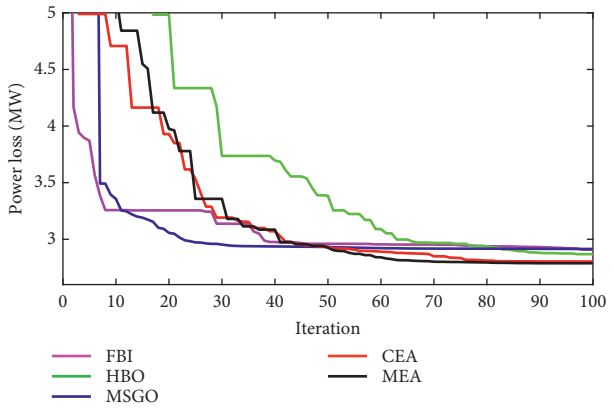

Figure 11: The best runs of methods for minimizing loss as placing one WPP at node 3.

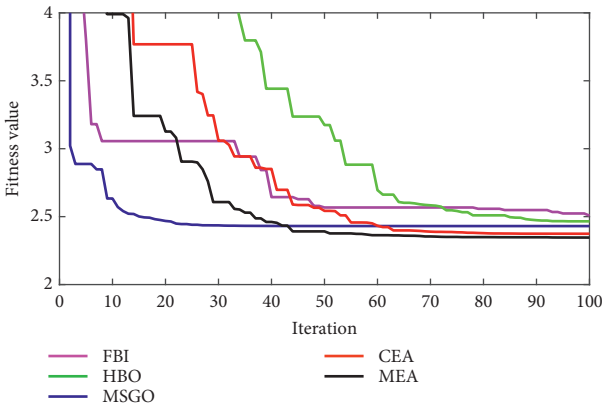

Figure 12: The best runs of methods for minimizing loss as placing one WPP at node 30.

control variables such as voltage and active power of THPs. Therefore, reaching optimal control parameters in the modified OPF problem becomes more difficult for metaheuristic algorithm. By experiment, MEA could solve the conventional OPF problem successfully for the IEEE 30-node system by setting 10 to population and 50 to iteration

Table 10: The results obtained by methods for placing one WPP at one unknown node.

Method	FBI	HBO	MSGO	CEA	MEA
Minimum power loss (MW)	2.70	2.49	2.46	2.45	2.39
Mean power loss (MW)	3.17	2.68	3.54	2.82	2.74
Maximum power loss (MW)	4.72	3.18	6.34	3.29	3.43
STD	0.40	0.13	0.97	0.21	0.21
N_1	10	30	15	30	30
N_3	100	100	100	100	100
Found position	30	30	30	30	30
Generation of WPP (MW)	8.8911	9.9998	9.9065	9.9855	9.9956
Power factor of WPP	0.9899	0.9503	0.9913	0.895	0.9122

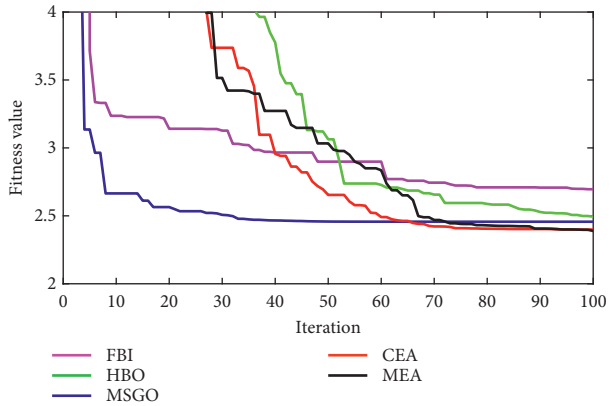

Figure 13: The best runs of five applied methods for Subcase 2.2.

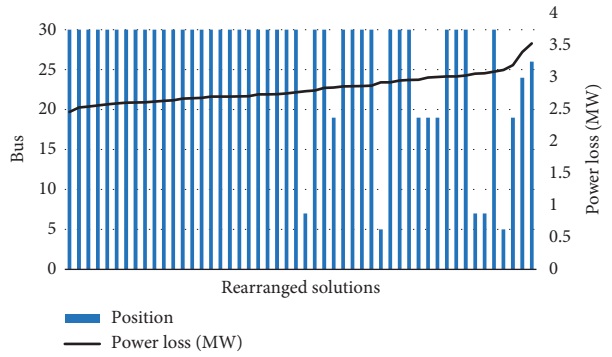

Figure 14: WPP location and loss of 50 rearranged runs obtained by MEA for Subcase 2.2.

number and MEA could reach the most optimal solutions by setting 15 to population and 75 to iteration number. However, for the modified problem with the placement of two WPPs, the settings to reach the best performance for MEA were 60 for population and 100 for the iteration number. Clearly, the setting values were higher for the modified OPF problem. About the average simulation time for the study cases, Table 13 summarizes the time from all methods for all study cases. Comparisons of the computation time indicate that MEA has the same computation time as FBI, HBO, MSGO, and CEA, but it has shorter time than JYA [47]. The average time for applied methods is about 30 seconds for the cases of placing one WPP and about 53 seconds for other cases of placing two WPPs, while the time is about 72 seconds for JYA for the cases of placing one WPP. The five algorithms approximately have the same average time because the setting of population and iteration number is the same. The reported time of the proposed method is not too long for a system with 30 nodes, and it seems that MEA can be capable for handling a real power system or a larger-scale power system. Therefore, we have tried to apply MEA for other larger scale systems with 57 or 118 nodes. For conventional OPF problem without the optimal placement of WPPs, MEA could solve the conventional OPF problem successfully. However, for the placement of WPPs in modified OPF problem for the IEEE 57-node system and the IEEE 118-node system, MEA could not succeed to reach valid solutions. Therefore, the highest shortcoming of the

Table 11: The results obtained by five methods for Subcase 2.2.1.

Method	FBI	HBO	MSGO	CEA	MEA
Minimum power loss (MW)	2.37	2.43	2.32	2.28	2.26
Mean power loss (MW)	2.60	2.57	2.64	2.49	2.51
Maximum power loss (MW)	2.97	2.85	3.30	2.85	2.89
STD	0.14	0.09	0.25	0.13	0.13
N_1	20	60	30	60	60
N_3	100	100	100	100	100
Location of WPPs	3, 30	3, 30	3, 30	3, 30	3, 30
Generation of WPPs (MW)	9.6108, 9.8128	7.4719, 9.9936	6.8908, 9.9674	9.8404, 9.9999	9.9922, 9.9299
Power factor of WPPs	0.9814, 0.9729	0.9925, 0.9352	0.8752, 0.9841	0.9974, 0.9542	0.8597, 0.9973

Table 12: The results obtained by five methods for Subcase 2.2.2.

Method	FBI	HBO	MSGO	CEA	MEA
Minimum power loss (MW)	2.24	2.16	2.10	2.05	2.03
Mean power loss (MW)	2.61	2.37	2.46	2.27	2.31
Maximum power loss (MW)	3.93	2.64	4.24	2.70	2.77
STD	0.28	0.13	0.37	0.15	0.14
N_1	20	60	30	60	60
N_3	100	100	100	100	100
Locations of WPPs	30, 19	19, 30	30, 19	30, 19	24, 30
Generation of WPPs (MW)	9.83, 9.28	9.98, 9.97	9.70, 8.15	9.99, 9.98	9.95, 9.99
Power factor of WPPs	0.98, 0.96	1.00, 0.96	1.00, 0.92	0.94, 0.88	0.87, 0.99

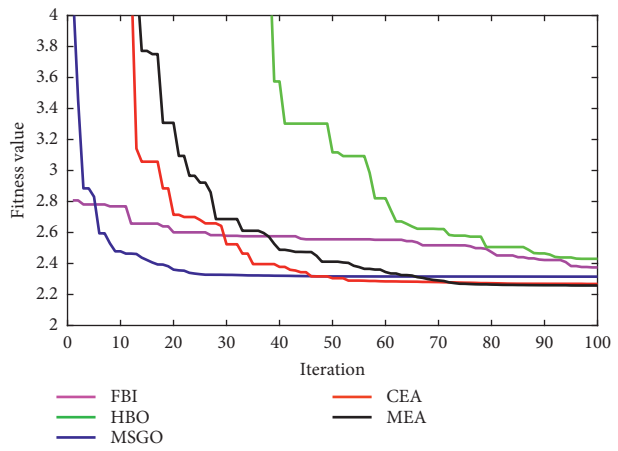

Figure 15: The best runs obtained by methods for Subcase 2.2.1.

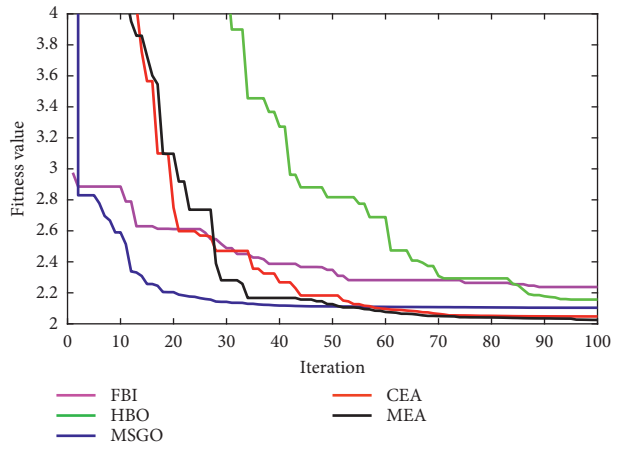

Figure 16: The best runs obtained by methods for Subcase 2.2.2.

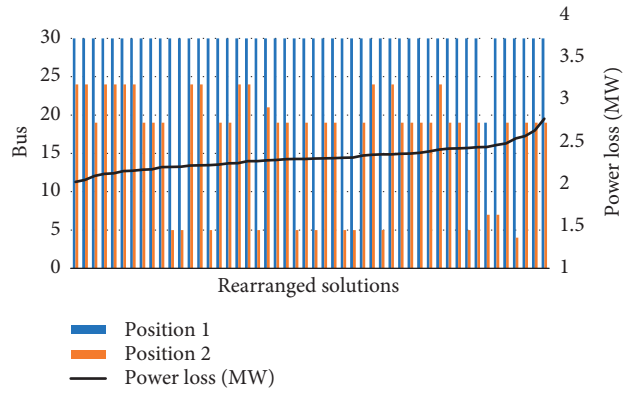

Figure 17: Power losses and locations of two WPPs for 50 runs obtained by MEA.

Table 13: Average computation time of each run obtained by methods for study cases.

Method	FBI	HBO	MSGO	CEA	MEA	JYA [47]
Case 1.1 (place one WPP at node 3)	35.21	30.65	32.82	28.18	28.45	~72.4
Case 1.1 (place one WPP at node 30)	28.93	26.06	32.45	27.07	27.77	~72.4
Case 1.2 (place one WPP at one unknown node)	27.93	31.92	27.32	27.64	27.76	—
Subcase 1.3.1 (place two WPPs at nodes 3 and 30)	51.04	53.36	53.56	53.38	52.57	—
Subcase 1.3.2 (place two WPPs at two unknown nodes)	55.18	54.05	56.27	54.18	55.14	—
Case 2.1 (place one WPP at node 3)	30.82	27.14	27.65	31.15	29.7	~72.4
Case 2.1 (place one WPP at node 30)	28.02	28.7	28.36	28.20	28.04	~72.4
Case 2.2 (place one WPP at one unknown node)	28.20	26.75	28.27	29.62	27.40	—
Subcase 2.2.1 (place two WPPs at nodes 3 and 30)	55.41	56.43	56.43	56.81	56.09	—
Subcase 2.2.2 (place one WPP at one unknown node)	54.04	54.14	59.2	55.19	56.12	—

study is not to reach the successful application of MEA for placing WPPs on large-scale systems with 57 and 118 nodes.

It can be stated that CEA and MEA are powerful optimization tools for the IEEE 30-node system, but their capability on other large-scale systems or real systems is limited. The methods may need more effective improvement to overcome the mentioned limitation.

6. Conclusions

In this paper, a modified OPF (MOPF) problem with the placement of wind power plants in an IEEE 30-bus transmission power network was solved by implementing four conventional metaheuristic algorithms and the proposed MEA. Two single objectives taken into account were minimization of total generation cost and minimization of power loss. About the number of WPPs located in the system, two cases are, respectively, one WPP and two WPPs. About the locations of the WPPs, simple cases were to accept the result from the previous study [47]. Buses 30 and 3 were the most effective and ineffective locations. The results indicated that the placement of one WPP at bus 30 can reach smaller power loss and smaller fuel cost than at bus 3. For other complicated cases, the paper also investigated the effectiveness of locations by applying MEA and four other metaheuristic algorithms to determine the locations. As a result, placing one WPP at bus 30 has reached the smallest power loss and the smallest total fuel cost. For placing two WPPs, buses 30 and 3 could not result in the smallest fuel cost and the smallest power loss. Buses 30 and 5 were the best locations for the minimization of fuel cost, while buses 30 and 24 were the best locations for the minimization of power loss. Therefore, the main contribution of the study regarding the electrical field is to determine the best locations for the best power loss and the best total cost.

For placing one WPP, fuel costs of MEA were the smallest and equal to \$764.33 and \$762.53 for locations at node 3 and node 30, whilst those of others were much higher and equal to \$769.963 and \$768.039, respectively. For placing two WPPs at two found locations, MEA has reached the cost of \$726.77, but the worst cost of others was \$728.81. The power losses of MEA were also reduced significantly as compared to others. For placing one WPP at node 3 and node 30, MEA has reached 2.79 and 2.35 MW, but those of others have been larger and equal to 3.339 and 2.67504 MW, respectively. For placing two WPPs at two found locations, the best loss of 2.03 MW was found by MEA and the worst loss of 2.24 MW was found by others. In summary, the proposed MEA could attain lesser cost than others from 0.28% to 0.73% and lesser power loss than others from 9.38% to 16.44%. Clearly, the improvement levels are significant. However, for other systems with larger scale, MEA could not succeed in determining the best location and size for WPPs. Thus, in the future work, we will find solutions to improve MEA for larger systems and real systems. In addition, we will also consider more renewable energy power plants, such as photovoltaic power plants and uncertainty characteristics of solar and wind speed. All considered complexities will form a real problem as a real power system, and contributions of optimization algorithms and renewable energies will be shown clearly.

Nomenclature

Fit_{mean}: Mean fitness of the available population
I_q, R_q: Current and resistance of the qth transmission line
N_{TG}: Quantity of thermal units
N_n: Quantity of nodes in networks
N_{LN}, N_{Br}: Quantity of load nodes and transmission lines
N_T: Quantity of transformers
N_1: Population
N_2: Number of control decision variables
N_3: The maximum iteration
N_W: Number of nodes with the presence of wind turbines
P_{TGi}, Q_{TGi}: Active and reactive power generation of the ith generator
P_{rqi}: Active power required by load at the ith node
$P_{TGi}^{\min}, P_{TGi}^{\max}$: Minimum and maximum output of active power generated by the ith generator
N_{Com}: Number of nodes with shunt capacitors
$Q_{TGi}^{\min}, Q_{TGi}^{\max}$: Minimum and maximum output of reactive power generated by the ith generator
Q_{TGx}: Reactive power generated by the thermal generator located at node x
Q_{rqx}: Reactive power required by load at node x
$Q_{\text{Com}x}$: Reactive power supplied by the compensator that actually is capacitor bank placed at node x
$Q_{\text{Com}x}^{\min}, Q_{\text{Com}x}^{\max}$: Minimum and maximum output of reactive power generated by shunt capacitors at node x
$P_{\text{Wind}}^{\min}$, $P_{\text{Wind}}^{\max}$, $Q_{\text{Wind}}^{\min}$, $Q_{\text{Wind}}^{\max}$: Minimum and maximum output of active and reactive power generated by wind turbines
r_1, r_2, r_3, r_4, r_5, r_6, r_7, r_8: Random number within 0 and 1
S_{Brq}: Operating apparent power of the qth line
$S_{Br}^{\max}$: Maximum limit of apparent power of the qth line
Tap_i: Selected tap of the transformer i
$\text{Tap}^{\min}$, $\text{Tap}^{\max}$: The lowest and highest tap settings of transformers
U_x, U_y: The voltage magnitudes at node x and node y
U_{TGi}: Voltage of the ith generator
$U_{TGi}^{\min}, U_{TGi}^{\max}$: Minimum and maximum voltage of the ith generator
U_{LNt}: Operating voltage of the tth load
$U_{LN}^{\min}$, $U_{LN}^{\max}$: Minimum and maximum operating voltage of loads
Y_{xy}: The admittance value between node x and node y
μ_1, μ_2, μ_3: Electricity generation cost coefficient
φ_x, φ_x: The voltage phasors at node x and node y
Z_{r1}, Z_{r2}, Z_{r3}, Z_{r4}: Randomly chosen solutions from population
AFAPA: Adaptive fuzzy artificial physics algorithm
AA: Antlion algorithm
APDE: Adaptive parameters based differential evolution
ACA: Ant colony algorithm
ABA: Artificial bee algorithm
APO: Artificial physics algorithm
ALPOS: Aging leader-based particle swarm optimization
BFA: Bacteria foraging algorithm
BSA: Bird swarm algorithm
BWOA: Black widow optimization algorithm
BMA: Barnacles mating algorithm
BA: Bat algorithm
BSA: Backtracking search algorithm
CSA1: Crow search algorithm
CSA: Cuckoo search algorithm
DE: Differential evolution
EGC: Electricity generation cost
FPA: Flower pollination algorithm
GSO: Glowworm swarm algorithm
GWA: Grey wolf algorithm
GSA: Gravitational search algorithm
GA: Genetic algorithm
HABC: Hybrid artificial bee colony algorithm
HA: Hybrid algorithm
HGTPEA: Hybrid genetic and two-point estimation algorithm
HGNIPA: Hybrid genetic and nonlinear interior point algorithm
HSQTIICA: Hybrid sequential quadratic technique and improved imperialist competitive algorithm
IMVA: Improved multiverse algorithm
IMA: Ion motion algorithm
IICA: Improved imperialist competitive algorithm
JYA: JAYA algorithm
KHA: Krill herd algorithm
MBFA: Modified bacteria foraging algorithm
MCS: Modified cuckoo search
MFO: Moth flame optimization
MHGSPSO: Modified hybrid gravitational search algorithm and particle swarm optimization
MVA: Multiverse algorithm
MFA: Moth flame algorithm
MJYA: Modified JAYA
MPSO: Modified particle swarm optimization
MDE: Modified differential evolution
MSA: Moth swarm algorithm
NSGA-II: Improved nondominated sorting genetic algorithm

NDSGWA: Nondominated sort grey wolf algorithm
PSO: Particle swarm optimization
RCGA: Real coded genetic algorithm
TUs: Thermal units
WTs: Wind turbines
WA: Whale algorithm
SSA: Salp swarm algorithm.

Data Availability

The input data for the IEEE 30-bus system in this study are available from the literature.

Conflicts of Interest

The authors declare that they have no conflicts of interest.

Acknowledgments

This research is funded by Vietnam National Foundation for Science and Technology Development (NAFOSTED) under grant number. 102.02-2020.07.

References

[1] L. Le Dinh, D. Vo Ngoc, and P. Vasant, "Artificial bee colony algorithm for solving optimal power flow problem," *The Science World Journal*, vol. 2013, Article ID 159040, 9 pages, 2013.

[2] L. Sun, J. Hu, and H. Chen, "Artificial bee colony algorithm based on *K*-means clustering for multiobjective optimal power flow problem," *Mathematical Problems in Engineering*, vol. 2015, Article ID 762853, 18 pages, 2015.

[3] R. Roy and H. T. Jadhav, "Optimal power flow solution of power system incorporating stochastic wind power using Gbest guided artificial bee colony algorithm," *International Journal of Electrical Power & Energy Systems*, vol. 64, pp. 562–578, 2015.

[4] G. Chen, S. Qiu, Z. Zhang, Z. Sun, and H. Liao, "Optimal power flow using gbest-guided cuckoo search algorithm with feedback control strategy and constraint domination rule," *Mathematical Problems in Engineering*, vol. 201714 pages, Article ID 9067520, 2017.

[5] T. L. Duong, N. A. Nguyen, and T. T. Nguyen, "A newly hybrid method based on cuckoo search and sunflower optimization for optimal power flow problem," *Sustainability*, vol. 12, no. 13, p. 5238, 2020.

[6] P. Umapathy, C. Venkataseshaiah, and M. S. Arumugam, "Particle swarm optimization with various inertia weight variants for optimal power flow solution," *Discrete Dynamics in Nature and Society*, vol. 2010, Article ID 462145, 15 pages, 2010.

[7] P. K. Roy, S. P. Ghoshal, and S. S. Thakur, "Multi-objective optimal power flow using biogeography-based optimization," *Electric Power Components and Systems*, vol. 38, no. 12, pp. 1406–1426, 2010.

[8] A.-F. Attia, Y. A. Al-Turki, and A. M. Abusorrah, "Optimal power flow using adapted genetic algorithm with adjusting population size," *Electric Power Components and Systems*, vol. 40, no. 11, pp. 1285–1299, 2012.

[9] R. Arul, G. Ravi, and S. Velusami, "Solving optimal power flow problems using chaotic self-adaptive differential harmony search algorithm," *Electric Power Components and Systems*, vol. 41, no. 8, pp. 782–805, 2013.

[10] H. R. E.-H. Bouchekara and M. A. Abido, "Optimal power flow using differential search algorithm," *Electric Power Components and Systems*, vol. 42, no. 15, pp. 1683–1699, 2014.

[11] H. R. El-Hana Bouchekara, M. A. Abido, and A. E. Chaib, "Optimal power flow using an improved electromagnetism-like mechanism method," *Electric Power Components and Systems*, vol. 44, no. 4, pp. 434–449, 2016.

[12] M. A. Taher, S. Kamel, F. Jurado, and M. Ebeed, "An improved moth-flame optimization algorithm for solving optimal power flow problem," *International Transactions on Electrical Energy Systems*, vol. 29, no. 3, Article ID e2743, 2019.

[13] M. A. Taher, S. Kamel, F. Jurado, and M. Ebeed, "Modified grasshopper optimization framework for optimal power flow solution," *Electrical Engineering*, vol. 101, no. 1, pp. 121–148, Article ID 0123456789, 2019.

[14] M. Pourakbari-Kasmaei, M. Lehtonen, M. Fotuhi-Firuzabad, M. Marzband, and J. R. S. Mantovani, "Optimal power flow problem considering multiple-fuel options and disjoint operating zones: a solver-friendly MINLP model," *International Journal of Electrical Power & Energy Systems*, vol. 113, pp. 45–55, 2019.

[15] K. Srilakshmi, P. Ravi Babu, and P. Aravindhababu, "An enhanced most valuable player algorithm based optimal power flow using Broyden's method," *Sustainable Energy Technologies and Assessments*, vol. 42, Article ID 100801, 2020.

[16] K. Nusair and F. Alasali, "Optimal power flow management system for a power network with stochastic renewable energy resources using golden ratio optimization method," *Energies*, vol. 13, no. 14, p. 3671, 2020.

[17] M. Z. Islam, N. I. A. Wahab, V. Veerasamy et al., "A harris hawks optimization based single- and multi-objective optimal power flow considering environmental emission," *Sustainability*, vol. 12, no. 13, p. 5248, 2020.

[18] S. Li, W. Gong, L. Wang, X. Yan, and C. Hu, "Optimal power flow by means of improved adaptive differential evolution," *Energy*, vol. 198, Article ID 117314, 2020.

[19] E. Naderi, M. Pourakbari-Kasmaei, F. V. Cerna, and M. Lehtonen, "A novel hybrid self-adaptive heuristic algorithm to handle single- and multi-objective optimal power flow problems," *International Journal of Electrical Power & Energy Systems*, vol. 125, Article ID 106492, 2021.

[20] M. Z. Islam, N. I. Abdul Wahab, V. Veerasamy et al., "Generation fuel cost and loss minimization using salp swarm algorithm based optimal power flow," in *Proceedings of the 2020 International Conference on Computer Communication and Informatics*, pp. 1–6, Coimbatore, India, January 2020.

[21] P. P. Biswas, P. N. Suganthan, R. Mallipeddi, and G. A. J. Amaratunga, "Optimal power flow solutions using differential evolution algorithm integrated with effective constraint handling techniques," *Engineering Applications of Artificial Intelligence*, vol. 68, pp. 81–100, 2018.

[22] G. Chen, Z. Lu, and Z. Zhang, "Improved krill herd algorithm with novel constraint handling method for solving optimal power flow problems," *Energies*, vol. 11, no. 1, p. 76, 2018.

[23] A. Khelifi, B. Bentouati, and S. Chettih, "Optimal power flow problem solution based on hybrid firefly krill herd method," *International Journal of Engineering Research in Africa*, vol. 44, pp. 213–228, 2019.

[24] A. Alhejji, M. Ebeed Hussein, S. Kamel, and S. Alyami, "Optimal power flow solution with an embedded center-node unified power flow controller using an adaptive grasshopper

optimization algorithm," *IEEE Access*, vol. 8, pp. 119020–119037, 2020.

[25] A. Panda and M. Tripathy, "Optimal power flow solution of wind integrated power system using modified bacteria foraging algorithm," *International Journal of Electrical Power & Energy Systems*, vol. 54, pp. 306–314, 2014.

[26] A. Panda and M. Tripathy, "Security constrained optimal power flow solution of wind-thermal generation system using modified bacteria foraging algorithm," *Energy*, vol. 93, pp. 816–827, 2015.

[27] X. Hao, C. Jiang, L. Wu, and L. Zhang, "Based on the power factors of dfig wind farm for power flow optimization," *Proceedings of the Second International Conference on Mechatronics and Automatic Control*, vol. 334, pp. 157–165, 2015.

[28] C. Mishra, S. P. Singh, and J. Rokadia, "Optimal power flow in the presence of wind power using modified cuckoo search," *IET Generation, Transmission & Distribution*, vol. 9, no. 7, pp. 615–626, 2015.

[29] A. Panda and M. Tripathy, "Solution of wind integrated thermal generation system for environmental optimal power flow using hybrid algorithm," *Journal of Electrical Systems and Information Technology*, vol. 3, no. 2, pp. 151–160, 2016.

[30] S. B. Pandya and H. R. Jariwala, "Stochastic wind-thermal power plants integrated multi-objective optimal power flow," *Majlesi Journal of Electrical Engineering*, vol. 14, no. 2, pp. 93–110, 2020.

[31] K. Teeparthi and D. M. Vinod Kumar, "Security-constrained optimal power flow with wind and thermal power generators using fuzzy adaptive artificial physics optimization algorithm," *Neural Computing and Applications*, vol. 29, no. 3, pp. 855–871, 2018.

[32] A. Abdollahi, A. Ghadimi, M. Miveh, F. Mohammadi, and F. Jurado, "Optimal power flow incorporating facts devices and stochastic wind power generation using krill herd algorithm," *Electronics*, vol. 9, no. 6, p. 1043, 2020.

[33] S. R. Salkuti, "Optimal power flow using multi-objective glowworm swarm optimization algorithm in a wind energy integrated power system," *International Journal of Green Energy*, vol. 16, no. 15, pp. 1547–1561, 2019.

[34] S. Duman, J. Li, L. Wu, and U. Guvenc, "Optimal power flow with stochastic wind power and FACTS devices: a modified hybrid PSOGSA with chaotic maps approach," *Neural Computing and Applications*, vol. 32, no. 12, pp. 1–30, 2020.

[35] M. Ahmad, N. Javaid, I. A. Niaz, S. Shafiq, O. Ur Rehman, and H. Majid Hussain, *Application of Bird Swarm Algorithm for Solution of Optimal Power Flow Problems*, Springer International Publishing, Berlin, Germany, 2019.

[36] M. Abdullah, N. Javaid, A. Chand, and Z. A. Khan, *Multi-objective Optimal Power Flow Using Improved Multi-Objective Multi-Verse Algorithm*, Springer International Publishing, Berlin, Germany, 2019.

[37] T. Samakpong, W. Ongsakul, and M. Nimal Madhu, "Optimal power flow considering cost of wind and solar power uncertainty using particle swarm optimization," *Advances in Intelligent Systems and Computing*, vol. 1072, pp. 190–203, 2020.

[38] E. X. S. Araujo, M. C. Cerbantes, and J. R. S. Mantovani, "Optimal power flow with renewable generation: a modified NSGA-II-based probabilistic solution approach," *Journal of Control, Automation and Electrical Systems*, vol. 31, no. 4, pp. 979–989, 2020.

[39] S. B. Pandya and H. R. Jariwala, "Stochastic renewable energy resources integrated multi-objective optimal power flow," *TELKOMNIKA (Telecommunication Computing Electronics and Control)*, vol. 18, no. 3, pp. 1582–1599, 2020.

[40] I. U. Khan, N. Javaid, K. A. A. Gamage, C. J. Taylor, S. Baig, and X. Ma, "Heuristic algorithm based optimal power flow model incorporating stochastic renewable energy sources," *IEEE Access*, vol. 8, pp. 148622–148643, 2020.

[41] M. H. Sulaiman and Z. Mustaffa, "Optimal power flow incorporating stochastic wind and solar generation by metaheuristic optimizers," *Microsystem Technologies*, vol. 27, no. 9, pp. 1–15, 2020.

[42] F. Daqaq, M. Ouassaid, R. Ellaia, and A. T. Zeine, "Optimal power flow solution including stochastic renewable resources," in *Proceedings of the 2018 6th International Renewable and Sustainable Energy Conference (IRSEC)*, pp. 1–6, Rabat, Morocco, December 2018.

[43] P. P. Biswas, P. N. Suganthan, and G. A. J. Amaratunga, "Optimal power flow solutions incorporating stochastic wind and solar power," *Energy Conversion and Management*, vol. 148, pp. 1194–1207, 2017.

[44] S. S. Reddy, "Optimal power flow with renewable energy resources including storage," *Electrical Engineering*, vol. 99, no. 2, pp. 685–695, 2017.

[45] J. Jiang, X. Han, J. Wang, X. Zhu, D. Sun, and Y. Ma, "Optimal power flow with transmission switching for power system with wind/photovoltaic generation," in *Proceedings of the 2017 Chinese Automation Congress, CA*, pp. 5802–5806, Jinan, China, October 2017.

[46] S. B. Pandya and H. R. Jariwala, "Renewable energy resources integrated multi-objective optimal power flow using non-dominated sort grey wolf optimizer," *Journal of Green Engineering*, vol. 10, no. 1, pp. 180–205, 2020.

[47] W. Warid, H. Hizam, N. Mariun, and N. Abdul-Wahab, "Optimal power flow using the Jaya algorithm," *Energies*, vol. 9, no. 9, p. 678, 2016.

[48] J. Ben Hmida, T. Chambers, and J. Lee, "Solving constrained optimal power flow with renewables using hybrid modified imperialist competitive algorithm and sequential quadratic programming," *Electric Power Systems Research*, vol. 177, Article ID 105989, 2019.

[49] E. E. Elattar and S. K. ElSayed, "Modified JAYA algorithm for optimal power flow incorporating renewable energy sources considering the cost, emission, power loss and voltage profile improvement," *Energy*, vol. 178, pp. 598–609, 2019.

[50] M. Zhang and Y. Li, "Multi-objective optimal reactive power dispatch of power systems by combining classification-based Multi-objective evolutionary algorithm and integrated decision making," *IEEE Access*, vol. 8, pp. 38198–38209, 2020.

[51] V. Suresh and S. S. Kumar, "Optimal reactive power dispatch for minimization of real power loss using SBDE and DE-strategy algorithm," *Journal of Ambient Intelligence and Humanized Computing*, pp. 1–15, 2020, In press.

[52] Y. Li and Y. Li, "Security-constrained multi-objective optimal power flow for a hybrid AC/VSC-MTDC system with lasso-based contingency filtering," *IEEE Access*, vol. 8, pp. 6801–6811, 2018.

[53] Y. Li, Y. Li, G. Li, D. Zhao, and C. Chen, "Two-stage multi-objective OPF for AC/DC grids with VSC-HVDC: incorporating decisions analysis into optimization process," *Energy*, vol. 147, pp. 286–296, 2018.

[54] A. Faramarzi, M. Heidarinejad, B. Stephens, and S. Mirjalili, "Equilibrium optimizer: a novel optimization algorithm," *Knowledge-Based Systems*, vol. 191, Article ID 105190, 2020.

[55] D. T. Abdul-hamied, A. M. Shaheen, W. A. Salem, W. I. Gabr, and R. A. El-sehiemy, "Equilibrium optimizer based multi

dimensions operation of hybrid AC/DC grids," *Alexandria Engineering Journal*, vol. 59, no. 6, pp. 4787–4803, 2020.

[56] A. M. Shaheen, A. M. Elsayed, R. A. El-Sehiemy, and A. Y. Abdelaziz, "Equilibrium optimization algorithm for network reconfiguration and distributed generation allocation in power systems," *Applied Soft Computing*, vol. 98, Article ID 106867, 2021.

[57] H. Ozkaya, M. Yıldız, A. R. Yıldız, S. Bureerat, B. S. Yıldız, and S. M. Sait, "The equilibrium optimization algorithm and the response surface-based metamodel for optimal structural design of vehicle components," *Materials Testing*, vol. 62, no. 5, pp. 492–496, 2020.

[58] A. B. Krishna, S. Saxena, and V. K. Kamboj, "A novel statistical approach to numerical and multidisciplinary design optimization problems using pattern search inspired Harris hawks optimizer," *Neural Computing and Applications*, vol. 33, no. 12, pp. 7031–7072, 2021.

[59] M. Abdel-Basset, R. Mohamed, S. Mirjalili, R. K. Chakrabortty, and M. J. Ryan, "Solar photovoltaic parameter estimation using an improved equilibrium optimizer," *Solar Energy*, vol. 209, pp. 694–708, 2020.

[60] J. Zhao and Z. Gao, "The improved equilibrium optimization algorithm with best candidates," *Journal of Physics: Conference Series*, vol. 1575, no. 1, Article ID 012089, 2020.

[61] J. Zhao and Z. M. Gao, "The improved mayfly optimization algorithm with Chebyshev map," *Journal of Physics: Conference Series*, vol. 1684, pp. 343–346, 2020.

[62] A. Wunnava, M. K. Naik, R. Panda, B. Jena, and A. Abraham, "A novel interdependence based multilevel thresholding technique using adaptive equilibrium optimizer," *Engineering Applications of Artificial Intelligence*, vol. 94, Article ID 103836, 2020.

[63] Q. Askari, M. Saeed, and I. Younas, "Heap-based optimizer inspired by corporate rank hierarchy for global optimization," *Expert Systems with Applications*, vol. 161, Article ID 113702, 2020.

[64] J.-S. Chou and N.-M. Nguyen, "FBI inspired meta-optimization," *Applied Soft Computing*, vol. 93, Article ID 106339, 2020.

[65] A. Naik, S. C. Satapathy, and A. Abraham, "Modified social group optimization-a meta-heuristic algorithm to solve short-term hydrothermal scheduling," *Applied Soft Computing*, vol. 95, p. 106524, 2020.

[66] T. T. Nguyen, "A high performance social spider optimization algorithm for optimal power flow solution with single objective optimization," *Energy*, vol. 171, pp. 218–240, 2019.

[67] R. D. Zimmerman and C. E. Murillo-Sánchez: http://www.pserc.cornell.edu/matpower, 2017.